

考虑前屈曲耦合变形时功能梯度圆板的稳定性分析

戚鹏程, 马连生

兰州理工大学, 工程力学系, 甘肃 兰州
Email: 1437173953@qq.com, lsma@lut.cn

收稿日期: 2021年1月7日; 录用日期: 2021年3月5日; 发布日期: 2021年3月16日

摘要

功能梯度材料(FGM)结构的非均匀性来自于材料组份沿某一方向梯度变化, 因此会存在拉弯耦合效应。在周边简支边界条件下, 只要有面内载荷就会产生挠度。本文基于经典板理论, 研究了机械载荷和热载荷作用下FGM简支圆板的非线性变形及稳定性问题。假设FGM圆板的材料性质只沿厚度方向进行变化, 利用能量原理推导出FGM圆板的平衡方程, 得到了包含前屈曲耦合变形影响的控制方程, 并用打靶法进行求解。讨论了外载荷、前屈曲耦合变形以及材料的温度依赖性质等因素对FGM圆板非线性变形和稳定性的影响。

关键词

功能梯度圆板, 前屈曲耦合变形, 打靶法, 临界载荷, 稳定性

Stability Analysis of Functionally Graded Circular Plates Considering Pre-Buckling Coupling Deformation

Pengcheng Qi, Liansheng Ma

Department of Engineering Mechanics, Lanzhou University of Technology, Lanzhou Gansu
Email: 1437173953@qq.com, lsma@lut.cn

Received: Jan. 7th, 2021; accepted: Mar. 5th, 2021; published: Mar. 16th, 2021

Abstract

The inhomogeneity of functionally graded materials (FGM) structure comes from the gradient change of material components along a certain direction, so there will be stretch bending coupling effect. As long as the in-plane load is applied, deflection will occur, in the case of simply supported boundary conditions. Based on the classical plate theory, the nonlinear deformation and stability of FGM simply supported circular plates under mechanical and thermal loads are studied in this paper. Assuming that the material properties of FGM circular plate only change along the thickness direction, the equilibrium equation of FGM circular plate is derived by using the energy principle, and the governing equation including the influence of pre-buckling coupling deformation is obtained, which is solved by shooting method. The effects of external loads, pre-buckling coupling deformation and temperature dependence of material properties on the nonlinear deformation and stability of FGM circular plate are discussed.

Keywords

FGM Circular Plate, Pre-Buckling Coupling Deformation, Shooting Method, Critical Load, Stability

Copyright © 2021 by author(s) and Hans Publishers Inc.

This work is licensed under the Creative Commons Attribution International License (CC BY 4.0).

<http://creativecommons.org/licenses/by/4.0/>



Open Access

1. 引言

功能梯度材料是一种材料组分按梯度变化的新型材料,因其优异性能被广泛关注。关于 FGM 结构稳定性分析的研究结果已经十分丰富。基于 Love-Kirchhoff 假设和 Sander 非线性应变位移关系, Najafizadeh 和 Eslami [1]研究了受均匀径向压力的简支和夹紧 FGM 圆板的屈曲问题。几年后, Najafizadeh 和 Heydari [2]又给出了基于高阶剪切变形理论的封闭解。Ma 和 Wang [3] [4]分析了 FGM 圆板的弯曲和过屈曲,发现 FGM 的过屈曲行为不同于均匀板。对于具有任意材料特性的 FGM 板的后屈曲行为, Lal 等[5]得到了后屈曲响应的二阶统计量。而 Li 等[6]通过打靶法数值求解,直接得到了有几何缺陷的 FGM 圆板的非线性热-机械载荷后屈曲响应。Samsam 等[7]和 Mohammadi 等[8]研究了 FGM 矩形薄板的屈曲问题。利用有限元方法, Ghomshei 和 Abbasi [9]分析了变厚度 FGM 圆环板的热屈曲。后来,李清禄等[10]研究了变厚度 FGM 圆板的热后屈曲,结果表明径向厚度的变化并不会影响热临界载荷值,但会影响屈曲以后的平衡路径。而 Zhao [11]发现,当热载荷和机械载荷的值以及它们的加载顺序满足一定的组合时,固支圆板不可避免地会发生二次屈曲(跳跃屈曲)。最近, Trinh 等[12]给出了多孔 FGM 板随机屈曲的封闭形式的临界载荷,也有一些研究人员[13] [14]分析了裂纹对 FGM 板稳定性的影响。

FGM 结构由于具有非均匀性,在简支边界条件下会引起前屈曲耦合变形,即只要面内载荷存在,就产生耦合挠度。这种情形下, FGM 简支圆板的屈曲问题变得十分复杂,与均匀材料圆板有着显著的区别 [3] [4] [15] [16]。本文中屈曲是指面内载荷有微小变化就会引起圆板挠度的大幅度增加或减小,在其载荷-挠度曲线上出现一个“平台” [15] [16] [17]。杨帆和马连生[18]的研究结果表明,前屈曲耦合变形对 FGM 圆板的稳定性确实有一定影响。而过去的一些研究成果没有考虑前屈曲耦合变形,掉进了 Quta 和 Leissa [15] [16]所称的“陷阱”,这个观点也被很多研究人员的成果[3] [19] [20] [21] [22] [23]所证实。

据作者所知, 关于前屈曲耦合变形对 FGM 结构稳定性影响的研究成果很少见于报道。本文将在文献[18]的基础上, 进一步研究面内载荷作用下 FGM 简支圆板的稳定性问题, 讨论前屈曲耦合变形、外载荷和材料的温度依赖性质等因素对 FGM 圆板稳定性的影响。

2. 基本方程

研究一个半径为 b , 厚度为 h 的 FGM 圆板, 设板承受均布径向压力 p 或受可沿板厚度方向变化的热场作用。假设材料组分只沿厚度方向变化, 并且材料性质 P (弹性模量 E 、热膨胀系数 α 及热传导率 K 等) 可表示为:

$$P(z) = (P_c - P_m) \left(\frac{h+2z}{2h} \right)^n + P_m \quad (1)$$

这里, 下标 c 和 m 分别表示陶瓷和金属材料, 上标 n 是梯度指数。

具有温度依赖的材料性质 P 写为:

$$P = P_0 (P_1 T^{-1} + 1 + P_2 T + P_3 T^2 + P_4 T^3) \quad (2)$$

考虑以下一个稳态温度场, 设该温度场仅沿板的厚度方向变化:

$$-\frac{d}{dz} \left(K(z) \frac{dT(z)}{dz} \right) = 0 \quad (3)$$

式中, $T(h/2) = T_c$, $T(-h/2) = T_m$, 积分上式得到温度场:

$$T(z) = T_m + (T_c - T_m) \frac{\int_{-h/2}^z \frac{dz}{K(z)}}{\int_{-h/2}^{h/2} \frac{dz}{K(z)}} \quad (4)$$

经典板理论下的位移场:

$$U_r(r, z) = U(r) - zW_{,r}, U_z(r, z) = W(r) \quad (5)$$

这里, U 和 W 分别是板中面的径向位移和横向位移。

板的应变与位移关系:

$$\varepsilon_r = U_{,r} + \frac{(W_{,r})^2}{2} - zW_{,rr} = \varepsilon_r^0 + zk_r, \varepsilon_\theta = \frac{U}{r} - \frac{zW_{,r}}{r} = \varepsilon_\theta^0 + zk_\theta \quad (6)$$

内力位移关系为:

$$N_r = A_{11} \left(\frac{\partial U}{\partial r} + \nu \frac{U}{r} + \frac{1}{2} \left(\frac{\partial W}{\partial r} \right)^2 \right) - B_{11} \left(\frac{\partial^2 W}{\partial r^2} + \frac{\nu}{r} \frac{\partial W}{\partial r} \right) - N^T \quad (7a)$$

$$N_\theta = A_{11} \left(\nu \frac{\partial U}{\partial r} + \frac{U}{r} + \frac{\nu}{2} \left(\frac{\partial W}{\partial r} \right)^2 \right) - B_{11} \left(\nu \frac{\partial^2 W}{\partial r^2} + \frac{1}{r} \frac{\partial W}{\partial r} \right) - N^T \quad (7b)$$

$$M_r = B_{11} \left(\frac{\partial U}{\partial r} + \nu \frac{U}{r} + \frac{1}{2} \left(\frac{\partial W}{\partial r} \right)^2 \right) - D_{11} \left(\frac{\partial^2 W}{\partial r^2} + \frac{\nu}{r} \frac{\partial W}{\partial r} \right) - M^T \quad (7c)$$

$$M_\theta = B_{11} \left(\nu \frac{\partial U}{\partial r} + \frac{U}{r} + \frac{\nu}{2} \left(\frac{\partial W}{\partial r} \right)^2 \right) - D_{11} \left(\nu \frac{\partial^2 W}{\partial r^2} + \frac{1}{r} \frac{\partial W}{\partial r} \right) - M^T \quad (7d)$$

其中, A_{11} , B_{11} 和 D_{11} 分别是拉压刚度、耦合刚度和抗弯刚度, N^T 和 M^T 分别是热薄膜力和热弯矩:

$$(A_{11}, B_{11}, D_{11}) = \int_{-h/2}^{h/2} Q_{11}(1, z, z^2) dz, Q_{11} = \frac{E(z)}{1-\nu^2} \quad (8a)$$

$$(N^T, M^T) = \int_{-h/2}^{h/2} \frac{E(z)}{1-\nu} \alpha(z) T(z) (1, z) dz \quad (8b)$$

根据能量原理, 可以推出 FGM 圆板的平衡方程与边界条件, 其无量纲形式如下:

$$\frac{d}{dx} \left[\frac{1}{x} \frac{d}{dx} (xu) \right] + \left[\frac{dw}{dx} \frac{d^2 w}{dx^2} + \frac{1-\nu}{2x} \left(\frac{dw}{dx} \right)^2 \right] - F_1 \frac{d}{dx} \nabla^2 w = 0 \quad (9a)$$

$$\begin{aligned} \nabla^4 w - F_2 \left[\nu \frac{du}{dx} + \frac{u}{x} + \frac{\nu}{2} \left(\frac{dw}{dx} \right)^2 \right] \frac{1}{x} \frac{dw}{dx} - F_2 \left[\frac{du}{dx} + \nu \frac{u}{x} + \frac{1}{2} \left(\frac{dw}{dx} \right)^2 \right] \frac{d^2 w}{dx^2} \\ + F_3 \left[\left(\frac{d^2 w}{dx^2} \right)^2 + \frac{2\nu}{x} \frac{dw}{dx} \frac{d^2 w}{dx^2} + \frac{1}{x^2} \left(\frac{dw}{dx} \right)^2 \right] + \bar{N} \nabla^2 w = 0 \end{aligned} \quad (9b)$$

这里, $\nabla^2 = \frac{1}{x} \frac{d}{dx} \left(x \frac{d}{dx} \right)$, $\nabla^4 = \frac{1}{x} \frac{d}{dx} \left[x \frac{d}{dx} \left(\frac{1}{x} \frac{d}{dx} \left(x \frac{d}{dx} \right) \right) \right]$ 。

板中心处条件:

$$u = \frac{dw}{dx} = 0, \lim_{x \rightarrow 0} \left(\frac{d^3 w}{dx^3} + \frac{1}{x} \frac{d^2 w}{dx^2} \right) = 0 \quad (10)$$

周边简支边界条件:

$$u = w = 0, F_4 \left[\frac{du}{dx} + \frac{1}{2} \left(\frac{dw}{dx} \right)^2 \right] - \left(\frac{d^2 w}{dx^2} + \frac{\nu}{x} \frac{dw}{dx} \right) - \bar{M} = 0 \quad (11)$$

无量纲量如下:

$$\begin{aligned} x = \frac{r}{b}, w = \frac{W}{h}, u = \frac{Ub}{h^2}, F_1 = \frac{F_3}{F_2}, F_2 = \frac{A_{11} h^2}{\Omega}, F_3 = \frac{B_{11} h}{\Omega}, F_4 = \frac{B_{11} h}{D_{11}}, \\ \bar{N} = \frac{N^T b^2}{\Omega}, \bar{M} = \frac{M^T b^2}{D_{11} h}, \Omega = D_{11} - \frac{B_{11}^2}{A_{11}}, F_p = \frac{pb^2}{A_{11} h^2} \end{aligned}$$

求解上述问题, 可以得到 FGM 简支圆板的载荷 - 挠度曲线(图 1, 图 3, 图 5)。从这些图中可以发现, 在某些情况下(如图 5), 横向挠度随着热载荷的增加而增大, 不出现“平台”。从图 1 和图 3 均可以看到, 对于任一条载荷 - 挠度曲线, 在某个载荷数值附近, 只要载荷数值小幅增加, 挠度数值就会大幅增大。即外载荷的微小增加导致了圆板横向挠度的迅速增大, 这意味着相应 FGM 圆板的抗弯刚度急剧降低, 近乎于丧失对变形的抵抗能力。因此, 当这样一个“平台”出现时, 可以认为圆板发生了屈曲[17][18]。

下面分析前屈曲耦合变形对 FGM 简支圆板屈曲的影响。

设在外因素 F 作用下, FGM 圆板的位移为 (\bar{u}, \bar{w}) , 当外因素增加 ΔF 后, 位移变为:

$$u = \bar{u} + \Delta u, w = \bar{w} + \Delta w \quad (12)$$

将式(12)代入式(9), 并忽略掉高阶小量后, 得到关于 Δu , Δw 的线性方程:

$$\begin{aligned} &\nabla^4 \Delta w - F_2 \left[\nu \frac{d\Delta u}{dx} + \frac{\Delta u}{x} + \nu \frac{d\Delta w}{dx} \frac{d\bar{w}}{dx} \right] \frac{1}{x} \frac{d\bar{w}}{dx} - F_2 \left[\nu \frac{d\bar{u}}{dx} + \frac{\bar{u}}{x} + \frac{\nu}{2} \left(\frac{d\bar{w}}{dx} \right)^2 \right] \frac{1}{x} \frac{d\Delta w}{dx} \\ &- F_2 \left[\frac{d\Delta u}{dx} + \frac{\nu}{x} \Delta u + \frac{d\bar{w}}{dx} \frac{d\Delta w}{dx} \right] \frac{d^2 \bar{w}}{dx^2} - F_2 \left[\frac{d\bar{u}}{dx} + \frac{\nu}{x} \bar{u} + \frac{1}{2} \left(\frac{d\bar{w}}{dx} \right)^2 \right] \frac{d^2 \Delta w}{dx^2} \end{aligned} \quad (13a)$$

$$+ F_3 \left[\left(2 \frac{d^2 \bar{w}}{dx^2} \frac{d^2 \Delta w}{dx^2} \right) + \frac{2\nu}{x} \left(\frac{d\Delta w}{dx} \frac{d^2 \bar{w}}{dx^2} + \frac{d\bar{w}}{dx} \frac{d^2 \Delta w}{dx^2} \right) + \frac{2}{x^2} \frac{d\bar{w}}{dx} \frac{d\Delta w}{dx} \right] + \bar{N} \nabla^2 \Delta w = 0$$

$$\frac{d}{dx} \left[\frac{1}{x} \frac{d}{dx} (x \Delta u) \right] + \left[\frac{d^2 \bar{w}}{dx^2} \frac{d\Delta w}{dx} + \frac{d\bar{w}}{dx} \frac{d^2 \Delta w}{dx^2} + \frac{1-\nu}{2x} \frac{d\bar{w}}{dx} \frac{d\Delta w}{dx} \right] - F_1 \frac{d}{dx} \nabla^2 \Delta w = 0 \quad (13b)$$

结合具体的边界条件, 求出前屈曲耦合变形 \bar{u} 和 \bar{w} (其中含有待定的外载荷)。然后将其代入式(13), 并在关于 Δu 和 Δw 的齐次边界条件下, 利用 Δu 和 Δw 有非零解这一条件来确定临界屈曲载荷。显然, 所求出的临界屈曲载荷包含了满足式(9)的前屈曲耦合变形的影响。如果不存在非零解, 则说明该问题并无屈曲现象发生。

当仅考虑均匀径向压力时, 上式中令 $\bar{N} = 0$ 即可。

3. 数值结果与讨论

本文的分析以 Si_3N_4 和 SUS304 为例, 取泊松比 $\nu = 0.3$, 材料性质参数值见表 1。

Table 1. Temperature-dependent coefficients for ceramic (Si_3N_4) and metals (SUS304)

表 1. 陶瓷和金属的材料常数

Material	Properties	P_{-1}	P_0	P_1	P_2	P_3
Si_3N_4	E	0	348.43E9	-3.070E-4	2.160E-7	-8.946E-11
	α	0	5.8723E-6	9.095E-4	0	0
	K	0	13.727	-1.032E-3	5.466E-7	-7.876E-11
SUS304	E	0	201.04E9	3.079E-4	-6.534E-7	0
	α	0	12.33E-6	8.086E-4	0	0
	K	0	15.379	-1.264E-3	2.092E-6	-7.223E-10

3.1. 受机械载荷作用

我们先分析受均匀径向压力 p 的 FGM 简支圆板, 边界条件为:

$$\begin{aligned} w = 0, F_4 \left[\frac{du}{dx} + \nu \frac{u}{x} + \frac{1}{2} \left(\frac{dw}{dx} \right)^2 \right] - \left(\frac{d^2 w}{dx^2} + \frac{\nu}{x} \frac{dw}{dx} \right) &= 0 \\ \left[\frac{du}{dx} + \nu \frac{u}{x} + \frac{1}{2} \left(\frac{dw}{dx} \right)^2 \right] - F_1 \left(\frac{d^2 w}{dx^2} + \frac{\nu}{x} \frac{dw}{dx} \right) &= -F_p \end{aligned} \quad (14)$$

图 1 是均匀径向压力作用下的 FGM 简支可移圆板的载荷 - 挠度曲线。图中, 1 表示考虑前屈曲耦合变形, 0 表示未考虑前屈曲耦合变形。可以看出, 从载荷作用之初, 就有挠度产生, 但在载荷 - 挠度曲线上存在 quta 所称的“平台” [15] [16] [17]。数值结果也表明, 此种边界条件下 FGM 圆板的屈曲前变形是微小变形。因此, 我们可以将式(9)进行线性化:

$$\frac{d}{dx} \left[\frac{1}{x} \frac{d}{dx} (x\bar{u}) \right] - F_1 \frac{d}{dx} \nabla^2 \bar{w} = 0 \tag{15a-b}$$

$$\nabla^4 \bar{w} = 0$$

结合边界条件式(14)解得:

$$\bar{u} = -\lambda u_0 x, \bar{w} = \lambda w_0 (1 - x^2) \tag{16a-b}$$

将式(16)代入式(13), 可得包含前屈曲耦合变形影响的控制方程:

$$\frac{d^2 \Delta u}{dx^2} + \frac{1}{x} \frac{d \Delta u}{dx} - \frac{\Delta u}{x^2} - c_{n1} \frac{d^3 \Delta w}{dx^3} - c_{n1} \left(1 + \frac{c_{n2}}{1+\nu} \lambda x^2 \right) \frac{1}{x} \frac{d^2 \Delta w}{dx^2} + c_{n1} \left(1 - c_{n2} \frac{2-\nu}{1+\nu} \lambda x^2 \right) \frac{1}{x^2} \frac{d \Delta w}{dx} = 0 \tag{17a}$$

$$\frac{d^4 \Delta w}{dx^4} + \frac{2}{x} \frac{d^3 \Delta w}{dx^3} - \left[1 - c_{n2} (c_{n3} - 2c_{n4} (1+\nu)) \lambda x^2 + \frac{c_{n2}^2 c_{n4}}{2(1+\nu)} \lambda^2 x^4 \right] \frac{1}{x^2} \frac{d^2 \Delta w}{dx^2} + \left[1 + c_{n2} (c_{n3} - 2c_{n4} (1+\nu)) \lambda x^2 - \frac{c_{n2}^2 c_{n4} (2+3\nu)}{2(1+\nu)} \lambda^2 x^4 \right] \frac{1}{x^3} \frac{d \Delta w}{dx} + c_{n2} c_{n5} \lambda \left(\frac{d \Delta u}{dx} + \frac{\Delta u}{x} \right) = 0 \tag{17b}$$

这里,

$$D_c = \frac{E_c h^3}{12(1-\nu^2)}, \lambda = \frac{pb^2}{D_c}, c_{n1} = \frac{B_{11}}{A_1 h}, c_{n2} = \frac{D_c}{\Omega}, u_0 = \frac{D_{11} c_{n2}}{A_1 h^2 (1+\nu)},$$

$$w_0 = \frac{F_1 c_{n2}}{2(1+\nu)}, c_{n3} = \frac{D_{11}}{\Omega}, c_{n4} = \frac{B_{11}^2}{A_1 \Omega (1+\nu)}, c_{n5} = \frac{B_{11} h}{\Omega}$$

利用打靶法求解上式即可。

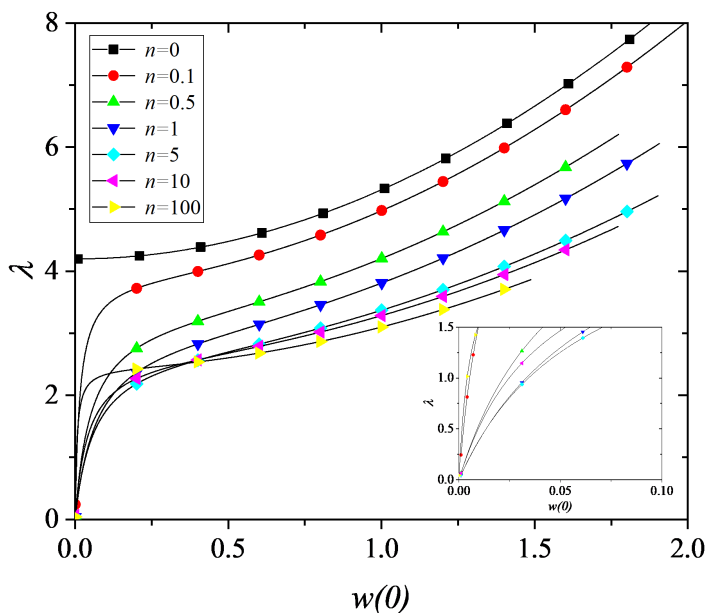


Figure 1. Load vs. deflection under mechanical load
图 1. 机械载荷下载荷 - 挠度曲线

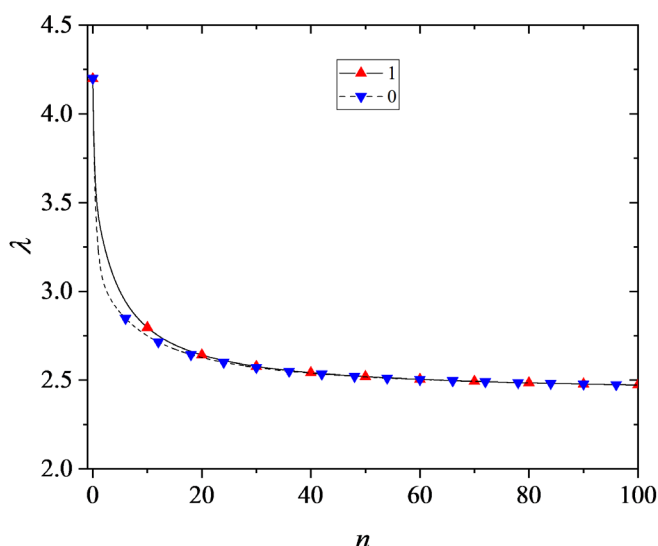


Figure 2. Critical load vs. gradient under mechanical load
图 2. 机械载荷下临界载荷随 n 变化曲线

图 2 是临界载荷随梯度指数变化的曲线，虚线参见文献[24]中的公式。可以看出，临界载荷随着 n 的增加而减小。这是因为 n 越大，金属的组分越多，陶瓷的组分越少，从而导致抗弯刚度减小，这与文献[25]的结论一致。并且，前屈曲耦合变形使得 FGM 圆板的临界载荷增大。

3.2. 受热载荷作用

考虑两种边界条件：

简支不可移：

$$u = w = 0, F_4 \left[\frac{du}{dx} + \frac{1}{2} \left(\frac{dw}{dx} \right)^2 \right] - \left(\frac{d^2 w}{dx^2} + \frac{\nu}{x} \frac{dw}{dx} \right) - \bar{M} = 0 \quad x = 1 \quad (18)$$

简支可移：

$$w = 0, \left[\frac{du}{dx} + \nu \frac{u}{x} + \frac{1}{2} \left(\frac{dw}{dx} \right)^2 \right] - F_1 \left(\frac{d^2 w}{dx^2} + \frac{\nu}{x} \frac{dw}{dx} \right) - \bar{N}_0 = 0, \quad x = 1 \quad (19)$$

$$F_4 \left[\frac{du}{dx} + \nu \frac{u}{x} + \frac{1}{2} \left(\frac{dw}{dx} \right)^2 \right] - \left(\frac{d^2 w}{dx^2} + \frac{\nu}{x} \frac{dw}{dx} \right) - \bar{M} = 0$$

这里， $\bar{N}_0 = \frac{N^T b^2}{A_{11} h^2}$ 。结合边界条件，利用打靶法可以得到热载荷作用下的载荷 - 挠度曲线。

图 3 是热载荷作用下，简支不可移 FGM 圆板的载荷挠度曲线，这里， $T_r = T_m / T_c$ 。实线表示考虑材料性质温度依赖性(TD)，虚线表示未考虑材料性质温度依赖性(TID)。从图可知，FGM 圆板在同一载荷下可能存在三种构形。受热载荷的简支不可移圆板的载荷 - 挠度曲线与夹紧圆板的载荷 - 挠度曲线[3]有明显的不同，夹紧边界的圆板发生典型的分支屈曲，而简支不可移的圆板出现了前屈曲耦合变形，这与受均匀径向压力的简支可移圆板的变形很相似，都出现了“平台” [17]。但随着圆板两侧的温差增大，即 T_r 越来越大或越来越小，“平台”越来越不明显。另外，在图 3(c)中， $n = 100$ 的曲线与其它曲线是不一样的。结合图 3(a)，图 3(b)，图 3(d)，我们发现，这是随着温差 T_r 变化，FGM 圆板的构形在发生翻转，

且均温时, $n = 100$ 的 FGM 圆板中陶瓷的材料组份非常大, 很难发生翻转。再者, 当均温时两个分支最接近, 温差越大, 两个分支距离越远。

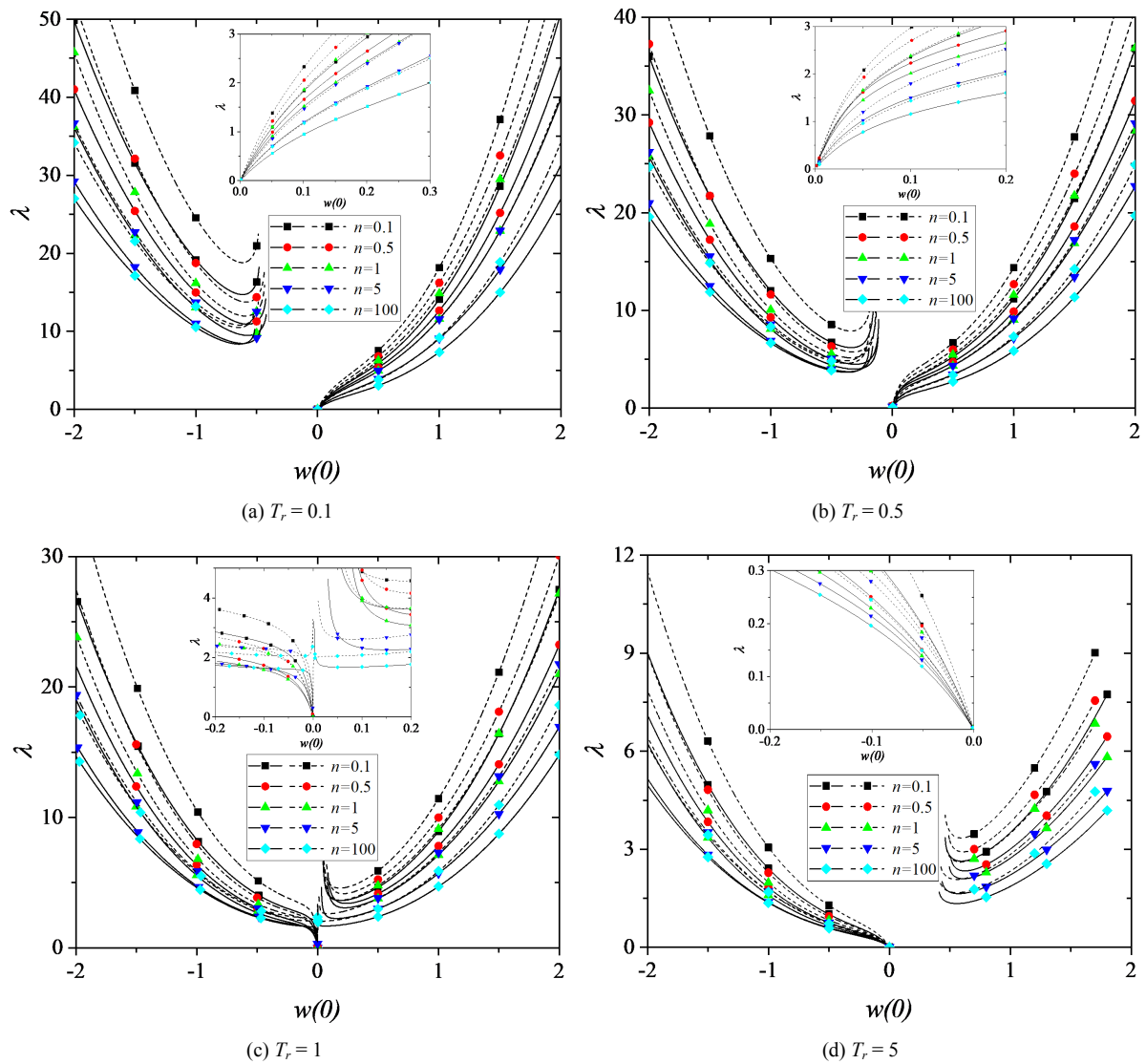


Figure 3. Load deflection curve of FGM simply supported and immovable circular plate under non-uniform thermal loads for different values of temperature ratio T_r .

图 3. 非均匀热载荷 FGM 简支不可移圆板载荷 - 挠度曲线

在均温或温差较小时, 前屈曲耦合挠度很明显, 且属于小变形, 因此, 我们可以将式(9)线性化:

$$\frac{d}{dx} \left[\frac{1}{x} \frac{d}{dx} (x\bar{u}) \right] - F_1 \frac{d}{dx} \nabla^2 \bar{w} = 0 \tag{20a}$$

$$\nabla^4 \bar{w} + \bar{N} \nabla^2 \bar{w} = 0 \tag{20b}$$

结合边界条件式(18)解得前屈曲耦合变形为:

$$\bar{u} = F_1 \beta A_0 (J_1(\beta)x - J_1(\beta x)), \bar{w} = A_0 (J_0(\beta x) - J_0(\beta)) \tag{21}$$

其中, $\beta = \sqrt{N}$, $A_0 = \frac{\bar{M}}{H}$, $H = (1 - F_1 F_4) \beta J_0(\beta) + \beta J_1(\beta)(\nu - 1 + 2F_1 F_4)$, 并且 J_0 和 J_1 分别为零阶第一类 Bessel 函数和一阶第一类 Bessel 函数。

将式(21)代入式(13), 可得热载荷作用下受前屈曲耦合变形影响的控制方程:

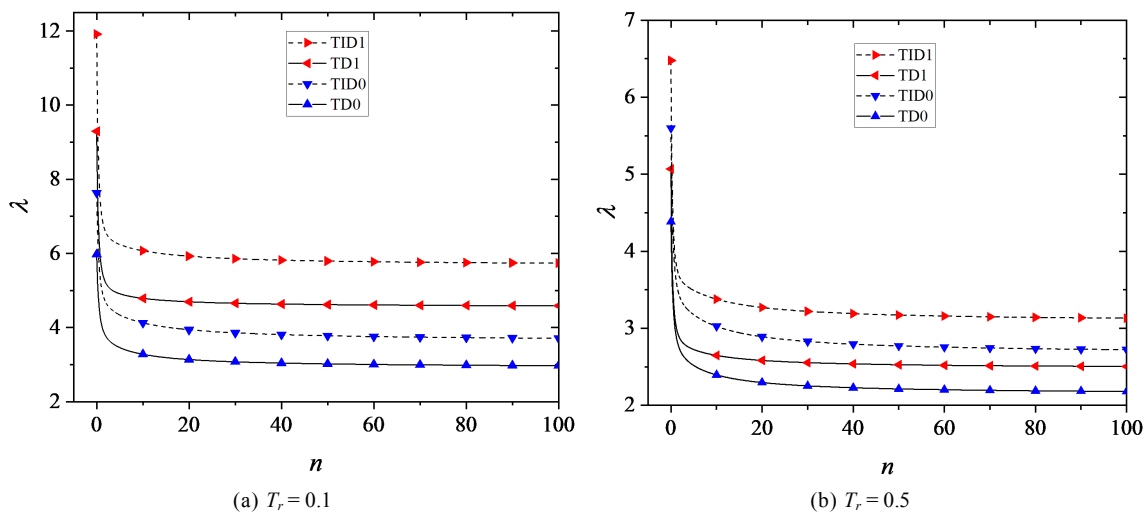
$$\frac{d^2 \Delta u}{dx^2} + \frac{1}{x} \frac{d \Delta u}{dx} - \frac{\Delta u}{x^2} - F_1 \frac{d^3 \Delta w}{dx^3} - (F_1 + x A_0 \beta J_1(\beta x)) \frac{1}{x} \frac{d^2 \Delta w}{dx^2} + \left[F_1 - x^2 A_0 \beta \left(J_0(\beta x) - \frac{\nu}{x} J_1(\beta x) \right) \right] \frac{1}{x^2} \frac{d \Delta w}{dx} = 0 \tag{22a}$$

$$\begin{aligned} & \frac{d^4 \Delta w}{dx^4} + \frac{2}{x} \frac{d^3 \Delta w}{dx^3} - \left[1 + x \beta A_0 J_1(\beta x) (F_1 F_2 - 2F_3) (1 - \nu) + \frac{1}{2} x^2 A_0^2 \beta^2 (J_1(\beta x))^2 \right] \frac{1}{x^2} \frac{d^2 \Delta w}{dx^2} \\ & - \left[-x^2 \beta A_0 (J_0(\beta x) (F_1 F_2 - 2F_3) - (1 + \nu) F_1 F_2 J_1(\beta)) \right] \frac{1}{x^2} \frac{d^2 \Delta w}{dx^2} \\ & + \left[1 + x \beta A_0 J_1(\beta x) (F_1 F_2 - 2F_3) (1 - \nu) + \frac{3\nu}{2} F_2 x^2 A_0^2 \beta^2 (J_1(\beta x))^2 \right] \frac{1}{x^3} \frac{d \Delta w}{dx} \\ & + \left[-x^2 ((1 + \nu) \beta A_0 F_1 F_2 J_1(\beta) - \nu \beta A_0 J_0(\beta x) (F_1 F_2 - 2F_3)) \right] \frac{1}{x^3} \frac{d \Delta w}{dx} \\ & - \left[F_2 A_0^2 \beta^2 J_1(\beta x) \left(J_0(\beta x) - \frac{1}{x} J_1(\beta x) \right) \right] \frac{d \Delta w}{dx} + \bar{N} \left(\frac{d^2 \Delta w}{dx^2} + \frac{1}{x} \frac{d \Delta w}{dx} \right) \\ & + \frac{F_2}{x} \beta A_0 J_1(\beta x) \left(\nu \frac{d \Delta u}{dx} + \frac{\Delta u}{x} \right) + F_2 \beta A_0 \left[J_0(\beta x) - \frac{1}{x} J_1(\beta x) \right] \left(\frac{d \Delta u}{dx} + \frac{\nu}{x} \Delta u \right) = 0 \end{aligned} \tag{22b}$$

利用打靶法求解即可得到热载荷作用下受前屈曲耦合变形影响的临界载荷。

图 4 是临界载荷随梯度指数变化曲线, 不考虑前屈曲耦合变形的数据参见文献[24]中的公式。数据表明, 前屈曲耦合变形对稳定性是有影响的。非均温时, 前屈曲耦合变形使得临界载荷增大, 而考虑材料性质温度依赖性会让临界载荷变小, 但依然大于不考虑前屈曲耦合变形时的临界载荷。均温时, 前屈曲耦合变形只在局部范围内对临界载荷有明显影响, 当 $n > 20$ 后, 几乎没有影响。随着 T_r 逐渐增大, 即陶瓷侧温度越来越低, 金属侧温度越来越高, FGM 圆板的临界载荷也在逐渐减小。

图 5 是热载荷作用下简支可移 FGM 圆板的载荷 - 挠度曲线。这是热弯曲线现象, 相同热载作用下, 考虑温度依赖性时产生的挠度更小, 这可能是因为温度依赖性减弱了拉弯耦合效应对挠度的影响。



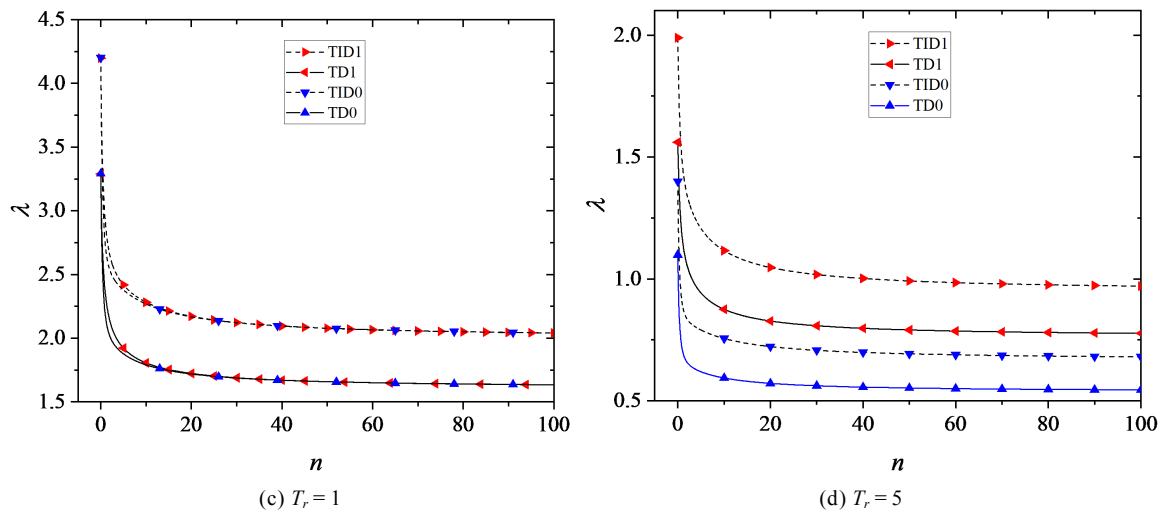


Figure 4. Critical load vs. gradient of FGM simply supported and immovable circular plate under non-uniform thermal load for different values of temperature ratio T_r

图 4. 非均匀热载荷下临界载荷随梯度指数 n 变化曲线

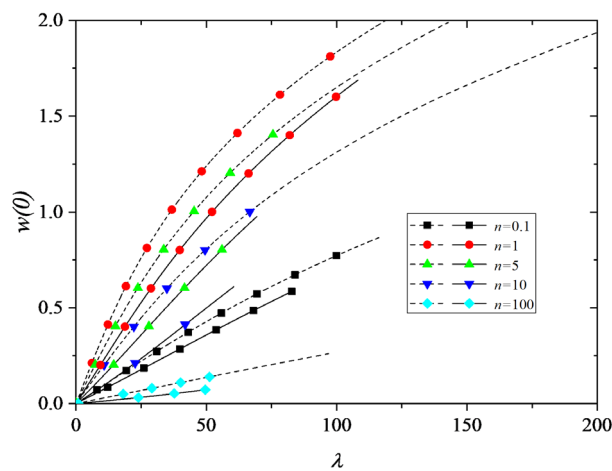


Figure 5. Load deflection curve of FGM simply supported and movable circular plate under uniform thermal load

图 5. 均温下 FGM 简支可移圆板载荷 - 挠度曲线

4. 结论

本文基于经典板理论, 研究了 FGM 简支圆板的非线性变形以及稳定性问题。推导了机械载荷和热载荷作用下, FGM 简支圆板受前屈曲耦合变形影响的控制方程, 分析了前屈曲耦合变形对 FGM 圆板稳定性的影响, 结果表明:

- 1) 机械载荷作用下, 考虑前屈曲耦合变形时, FGM 简支圆板的临界载荷增大。
- 2) 非均匀热载荷作用下, 简支不可移边界下 FGM 圆板的前屈曲耦合变形使得临界载荷增大; 而均温时, 前屈曲耦合变形只在局部范围内对临界载荷有明显影响。
- 3) 材料的温度依赖性质降低了 FGM 圆板的临界载荷。
- 4) 均温下的简支可移 FGM 圆板的挠度随着热载荷的增加而增大, 不出现“平台”, 只是通常意义上的弯曲。

- 5) 陶瓷侧温度越来越低, 金属侧温度越来越高时, FGM 圆板的临界载荷越小。
- 6) 同一热载荷下, FGM 圆板可能存在三种构形; 随着上下面的温差变化, FGM 圆板的构形会发生翻转。

基金项目

本文得到国家自然科学基金 11862012 和 12062010 的资助。

参考文献

- [1] Najafizadeh, M.M. and Eslami, M.R. (2002) Buckling Analysis of Circular Plates of Functionally Graded Materials under Uniform Radial Compression. *International Journal of Mechanical Sciences*, **44**, 2479-2493. [https://doi.org/10.1016/S0020-7403\(02\)00186-8](https://doi.org/10.1016/S0020-7403(02)00186-8)
- [2] Najafizadeh, M.M. and Heydari, H.R. (2008) An Exact Solution for Buckling of Functionally Graded Circular Plates Based on Higher Order Shear Deformation Plate Theory under Uniform Radial Compression. *International Journal of Mechanical Sciences*, **50**, 603-612. <https://doi.org/10.1016/j.ijmecsci.2007.07.010>
- [3] Ma, L.S. and Wang, T.J. (2003) Nonlinear Bending and Post-Buckling of a Functionally Graded Circular Plate under Mechanical and Thermal Loadings. *International Journal of Solids and Structures*, **40**, 3311-3330. [https://doi.org/10.1016/S0020-7683\(03\)00118-5](https://doi.org/10.1016/S0020-7683(03)00118-5)
- [4] Ma, L.S. and Wang, T.J. (2002) Axisymmetric Post-Buckling of a Functionally Graded Circular Plate Subjected to Uniformly Distributed Radial Compression. *Materials Science Forum*, **423-425**, 719-724.
- [5] Lal, A., Jagtap, K.R. and Singh, B.N. (2013) Post Buckling Response of Functionally Graded Materials Plate Subjected to Mechanical and Thermal Loadings with Random Material Properties. *Applied Mathematical Modelling*, **37**, 2900-2920. <https://doi.org/10.1016/j.apm.2012.06.013>
- [6] Li, S.R., Zhang, J.H. and Zhao, Y.G. (2007) Nonlinear Thermomechanical Post-Buckling of Circular FGM Plate with Geometric Imperfection. *Thin-Walled Structures*, **45**, 528-536. <https://doi.org/10.1016/j.tws.2007.04.002>
- [7] Samsam Shariata, B.A. and Eslami, M.R. (2007) Buckling of Thick Functionally Graded Plates under Mechanical and Thermal Loads. *Composite Structures*, **78**, 433-439. <https://doi.org/10.1016/j.compstruct.2005.11.001>
- [8] Mohammadi, M., Saidi, A.R. and Jomehzadeh, E. (2010) Levy Solution for Buckling Analysis of Functionally Graded Rectangular Plates. *Applied Composite Materials*, **17**, 81-93. <https://doi.org/10.1007/s10443-009-9100-z>
- [9] Ghomshei, M.M. and Abbasi, V. (2013) Thermal Buckling Analysis of Annular FGM Plate Having Variable Thickness under Thermal Load of Arbitrary Distribution by Finite Element Method. *Journal of Mechanical Science and Technology*, **27**, 1031-1039. <https://doi.org/10.1007/s12206-013-0211-y>
- [10] 李清禄, 段鹏飞, 张靖华. 陶瓷基 FGM 材料线形变厚度圆板的热后屈[J]. 航空材料学报, 2019, 39(1): 102-107.
- [11] Zhao, W.D. (2020) Nonlinear Axisymmetric Thermomechanical Response of FGM Circular Plates. *Journal of the Brazilian Society of Mechanical Sciences and Engineering*, **42**, Article No. 360. <https://doi.org/10.1007/s40430-020-02440-0>
- [12] Trinh, M.C., Mukhopadhyay, T. and Kim, S.E. (2020) A Semi-Analytical Stochastic Buckling Quantification of Porous Functionally Graded Plates. *Aerospace Science and Technology*, **105**, Article ID: 105928. <https://doi.org/10.1016/j.ast.2020.105928>
- [13] Minh, P.P. and Duc, N.D. (2019) The Effect of Cracks on the Stability of the Functionally Graded Plates with Variable-Thickness Using HSDT and Phase-Field Theory. *Composites Part B: Engineering*, **175**, Article ID: 107086. <https://doi.org/10.1016/j.compositesb.2019.107086>
- [14] Ghannadpour, S.A.M., Karimi, M. and Tornabene, F. (2019) Application of Plate Decomposition Technique in Nonlinear and Post-Buckling Analysis of Functionally Graded Plates Containing Crack. *Composite Structures*, **220**, 158-167. <https://doi.org/10.1016/j.compstruct.2019.03.025>
- [15] Qatu, M.S. and Leissa, A.W. (1993) Buckling or Transverse Deflections of Unsymmetrically Laminated Plates Subjected to In-Plane Loads. *AIAA Journal*, **31**, 189-194. <https://doi.org/10.2514/3.11336>
- [16] Laissa, A.W. (1986) Condition for Laminated Plates to Remain Flat under in Plane Loading. *Composite Structure*, **6**, 261-270. [https://doi.org/10.1016/0263-8223\(86\)90022-X](https://doi.org/10.1016/0263-8223(86)90022-X)
- [17] 周履, 范赋群. 复合材料力学[M]. 北京: 高等教育出版社, 1991.
- [18] 杨帆, 马连生. 前屈曲耦合变形对 FGM 圆板稳定性的影响[J]. 工程力学, 2010, 27(4): 68-72, 89.
- [19] Liew, K.M., Yang, J. and Kitipornchai, S. (2003) Postbuckling of Piezoelectric FGM Plates Subject to Ther-

- mo-Electro-Mechanical Loading. *International Journal of Solids and Structures*, **40**, 3869-3892. [https://doi.org/10.1016/S0020-7683\(03\)00096-9](https://doi.org/10.1016/S0020-7683(03)00096-9)
- [20] Shen, H.S. (2005) Postbuckling of FGM Plates with Piezoelectric Actuators under Thermo-Electro-Mechanical Loadings. *International Journal of Solids and Structures*, **42**, 6101-6121. <https://doi.org/10.1016/j.ijsolstr.2005.03.042>
- [21] Shen, H.S. and Li, S.R. (2008) Postbuckling of Sandwich Plates with FGM Face Sheets and Temperature-Dependent Properties. *Composites Part B: Engineering*, **39**, 332-344. <https://doi.org/10.1016/j.compositesb.2007.01.004>
- [22] Ma, L.S. and Lee, D.W. (2011) A Further Discussion of Nonlinear Mechanical Behavior for FGM Beams under In-Plane Thermal Loading. *Composite Structures*, **93**, 831-842. <https://doi.org/10.1016/j.compstruct.2010.07.011>
- [23] Fallah, F., Vahidipoor, M.K. and Nosier, A. (2015) Post-Buckling Behavior of Functionally Graded Circular Plates under Asymmetric Transverse and In-Plane Loadings. *Composite Structures*, **125**, 477-488. <https://doi.org/10.1016/j.compstruct.2015.02.018>
- [24] Ma, L.S. and Wang, T.J. (2004) Relationships between Axisymmetric Bending and Buckling Solutions of FGM Circular Plates Based on Third-Order Plate Theory and Classical Plate Theory. *International Journal of Solids and Structures*, **41**, 85-101. <https://doi.org/10.1016/j.ijsolstr.2003.09.008>
- [25] Li, Q.L. and Zhang, J.H. (2016) Vibration and Post-Buckling of a Functionally Graded Beam Subjected to Non-Conservative Forces. *Journal of Vibroengineering*, **8**, 4901-4913. <https://doi.org/10.21595/jve.2016.16824>